

柔性环己烷六酸和刚性草酸配体桥连的稀土配位聚合物的水热合成与结构研究

王 静* 徐 敏 苏婷婷

(广州大学化学化工学院, 广州 510006)

摘要: 草酸铽与水合环己烷六酸($\text{H}_6\text{L}^{\text{I}} \cdot \text{H}_2\text{O}$) (顺式椅式构型 L^{I} : a,e,a,e,a,e) 在水热条件下反应生成一种新颖的三维稀土配位聚合物 $[\text{Tb}_4(\text{L}^{\text{II}})(\text{ox})_3(\text{H}_2\text{O})_8]$ (L^{II} 为反式椅式构型: e,e,e,e,e,e ; ox 为草酸根), 通过元素分析和红外光谱对这个配位聚合物进行了表征。X 射线单晶衍射分析表明该配合物属于三斜晶系, $P\bar{1}$ 空间群, 晶胞参数为: $a=0.602\,03(4)\text{ nm}$, $b=1.082\,78(8)\text{ nm}$, $c=1.294\,46(9)\text{ nm}$, $\alpha=67.908\,0(10)^\circ$, $\beta=82.109\,0(10)^\circ$, $\gamma=83.887\,0(10)^\circ$, $V=0.773\,07(9)\text{ nm}^3$, $Z=2$ 。在这个配合物的形成中, 顺式构型的 $\text{H}_6\text{L}^{\text{I}}$ 配体发生构型转变形成 L^{II} 配体, L^{II} 配体采取 μ_8 -桥连模式将 Tb 离子连接成一个具有孔洞的二维(Tb-L^{II})配位层。由 μ_2 -和 μ_4 -桥连模式构成的一维(Tb-ox)链将二维(Tb-L^{II})层连接成一个具有孔道的三维配位框架, ox 配体和水分子通过配位作用和氢键作用填充在孔道中。

关键词: 稀土配位聚合物; 环己烷六酸; 草酸; 水热合成

中图分类号: O614.341

文献标识码: A

文章编号: 1001-4861(2011)04-0737-06

Hydrothermal Synthesis and Crystal Structure of a Novel Lanthanide Coordination Polymer Bridged by Flexible Cyclohexane-1,2,3,4,5,6-hexacarboxylate and Rigid Oxalate Ligands

WANG Jing* XU Min SU Ting-Ting

(School of chemistry and chemical engineering, Guangzhou University, Guangzhou 510006, China)

Abstract: Reaction of $\text{Tb}_2(\text{ox})_3 \cdot 6\text{H}_2\text{O}$ and cyclohexane-1,2,3,4,5,6-hexacarboxylic acid hydrate ($\text{H}_6\text{L}^{\text{I}} \cdot \text{H}_2\text{O}$) (*cis-chair* conformation L^{I} : a,e,a,e,a,e) resulted in formation of a novel three-dimensional lanthanide coordination polymer $[\text{Tb}_4(\text{L}^{\text{II}})(\text{ox})_3(\text{H}_2\text{O})_8]$ (*trans-chair* conformation L^{II} : e,e,e,e,e,e ; ox: oxalate) under hydrothermal condition, which was characterized by elemental analysis and IR. X-ray diffraction crystal structure analysis shows that the complex crystallizes in triclinic system, space group $P\bar{1}$ with $a=0.602\,03(4)\text{ nm}$, $b=1.082\,78(8)\text{ nm}$, $c=1.294\,46(9)\text{ nm}$, $\alpha=67.908\,0(10)^\circ$, $\beta=82.109\,0(10)^\circ$, $\gamma=83.887\,0(10)^\circ$, $V=0.773\,07(9)\text{ nm}^3$, $Z=2$. In the formation of the complex, the *cis-chair* $\text{H}_6\text{L}^{\text{I}}$ ligand transformed to the *trans-chair* L^{II} ligand, which adopts μ_8 -bridging mode connecting the Tb atoms to form two-dimensional (Tb-L^{II}) layers with channels. The one-dimensional (Tb-ox) chains bridged by μ_2 - and μ_4 -ox ligands link the (Tb-L^{II}) layers to generate a three-dimensional framework with channels, which were filled with ox ligands and water molecules through coordination and hydrogen interactions. CCDC: 790926.

Key words: lanthanide coordination polymer; cyclohexanehexacarboxylate; oxalate; hydrothermal synthesis

收稿日期: 2010-09-06。收修改稿日期: 2010-11-13。

国家自然科学基金(No.20901018)和广东省自然科学基金(No.9451009101003177)资助项目。

*通讯联系人。E-mail: wangjizhu@yahoo.com.cn

The crystal engineering of lanthanide complexes has attracted considerable attention over the past decade, not only due to their fascinating structural diversity and the intriguing topological networks^[1-2], but also due to the potential application in medicine, magnetism, bioinorganic chemistry and luminescence^[3-4]. As is well known, lanthanide ions have their high and variable coordination numbers and flexible coordination environments, which can provide unique impetus for discovery of unusual network topologies^[5-6]. Consequently, a variety of lanthanide coordination polymers with interesting architectures and topologies have been synthesized successfully^[7-8].

In order to construct multicarboxylate coordination frameworks, two main kinds of organic ligands are extensively studied, one is rigid ligands such as benzenepolycarboxylates and pyridinepolycarboxylates^[9-11], the other is flexible ligands, such as cyclohexanepolycarboxylate^[12-13]. Recently, cyclohexane-1,2,3,4,5,6-hexacarboxylic acid (H_6L , L stands for the ligand with different conformations) with versatile flexible conformations has been proved by us to act as excellent building blocks with charge and multi-connecting ability in the construction of functional coordination polymers^[14-18]. And in our recent work, we have investigated the coordination chemistry of the cyclohexanehexacarboxylic ligand and trapped its four conformations in different coordination polymers by carefully controlling the reaction conditions^[14-19]. As our continuing investigation on this interesting metal- H_6L system, we employed the lanthanide Tb(III) to react with the H_6L I (*cis-chair* conformation L^I : *a,e,a,e,a,e*) ligand to investigate the ligand flexible conformations. Herein, we report a novel three-dimensional lanthanide coordination polymer $[Tb_4(L^{II})(ox)_3(H_2O)_8]$ (trans-chair conformation L^{II} : *e,e,e,e,e,e*, ox: oxalate) bridged by flexible

cyclohexanehexacarboxylate and rigid oxalate ligands. The conformation of the cyclohexanehexacarboxylate ligand transformed from L^I to L^{II} (Scheme 1).

1 Experimental section

1.1 Materials and physical measurements

The starting material cyclohexanehexacarboxylic acid hydrate ($H_6L^I \cdot H_2O$) employed was commercially available and used as received without further purification. The C and H microanalyses were carried out with an Elementar Vario-EL CHNS elemental analyzer. The FTIR spectra were recorded from KBr tablets in the range 4 000~400 cm^{-1} on a Bio-Rad FTS-7 spectrometer.

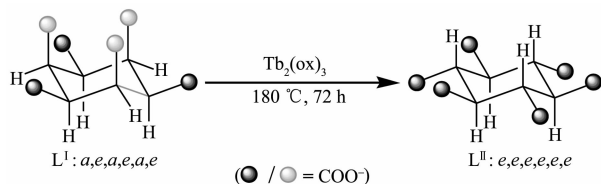
1.2 Hydrothermal synthesis

A mixture of $H_6L^I \cdot H_2O$ (0.087 g, 0.25 mmol) and $Tb_2(ox)_3 \cdot H_2O$ (0.345 g, 0.50 mmol) in H_2O (15 mL) were placed to a 25 mL Teflon reactor and heated in an oven to 180 $^{\circ}C$ for 72 h. After being cooled at a rate of ca. 5 $^{\circ}C \cdot h^{-1}$, the colorless crystals of the title complex in single phase (in ca. 15% yield based on H_6L^I) were obtained, isolated by filtration and washed with water. Elemental analysis calcd. for $C_9H_{11}O_{16}Tb_2$ (%): C 15.60, H 1.60; found (%): C 15.49, H 1.73. IR (KBr, 4 000~400 cm^{-1}): 3 429(s), 2 370(m), 1 686(s), 1 608(vs), 1 384(vs), 1 320(m), 1 262(w), 1 126(w), 1 041(w), 799(w), 619(w), 521(w).

1.3 Crystal structure determination

Data collections of the title complex were performed on a Bruker Smart Apex CCD diffractometer with Mo $K\alpha$ radiation ($\lambda=0.071\ 073$ nm) at 293(2) K. The raw data frames were integrated with SAINT⁺, and the corrections were applied for Lorentz and polarization effects. Absorption correction was applied by using the multiscan program SADABS^[20]. The structure was solved by direct methods, and all non-hydrogen atoms were refined anisotropically by least-squares on F^2 using the SHELXTL program^[21]. Hydrogen atoms on organic ligands were generated by the riding mode (C-H=0.093 nm). Crystal data as well as details of data collections and refinements for the complex are summarized in Table 1. Selected bond distances and bond angles are listed in Table 2.

CCDC: 790926.



Scheme 1 Summary of hydrothermal condition and ligand conformation transformation in the preparation of the title complex

Table 1 Crystal data and structure parameters for the title complex

Empirical formula	C ₉ H ₁₁ O ₁₆ Tb ₂	Absorption coefficient / mm ⁻¹	9.166
Formula weight	693.02	<i>F</i> (000)	646
Temperature / K	293(2)	Crystal size / mm	0.15×0.11×0.09
Wavelength / nm	0.071 073	θ range for data collection / (°)	1.71~26.00
Crystal system	Triclinic	Limiting indices	$-7 \leq h \leq 7, -13 \leq k \leq 13, -15 \leq l \leq 15$
Space group	<i>P</i> $\bar{1}$	Reflections collected	6 100
<i>a</i> / nm	0.602 03(4)	Independent reflections (<i>R</i> _{int})	3 017 (0.017 1)
<i>b</i> / nm	1.082 78(8)	Completeness / %	98.7
<i>c</i> / nm	1.294 46(9)	Max. and min. transmission	0.432 1 and 0.274 8
α / (°)	67.908 0(10)	Refinement method	Full-matrix least-squares on <i>F</i> ²
β / (°)	82.109 0(10)	Data / restraints / parameters	3 017 / 16 / 270
γ / (°)	83.887 0(10)	Goodness-of-fit on <i>F</i> ²	1.083
Volume / nm ³	0.773 07(9)	Final <i>R</i> indices (<i>I</i> >2σ(<i>I</i>))	<i>R</i> ₁ ^a =0.032 5, <i>wR</i> ₂ ^a =0.126 0
<i>Z</i>	2	<i>R</i> indices (all data)	<i>R</i> ₁ ^a =0.034 9, <i>wR</i> ₂ ^a =0.128 9
<i>D</i> _c / (g·cm ⁻³)	2.977	Largest diff. peak and hole / (e·nm ⁻³)	1 611, -1 070

$$^a R_1 = \sum \|F_o\| - |F_c| / \sum |F_o|, ^b wR_2 = [\sum w(F_o^2 - F_c^2)^2 / \sum w(F_o^2)^2]^{1/2}.$$

Table 2 Bond lengths (nm) and angles (°) for the title complex

Tb1-O5A	0.227 4(5)	Tb1-O2	0.248 7(6)	Tb2-O4W	0.239 4(6)
Tb1-O11	0.237 4(5)	Tb1-O12B	0.251 5(5)	Tb2-O 4D	0.2386(6)
Tb1-O9	0.239 8(6)	Tb1-O12C	0.252 8(8)	Tb2-O2W	0.241 0(7)
Tb1-O1W	0.241 6(7)	Tb2-O6D	0.229 8(6)	Tb2-O3W	0.244 0(6)
Tb1-O1	0.245 1(5)	Tb2-O3E	0.236 9(6)	Tb2-O10	0.244 7(5)
Tb1-O7	0.246 8(5)	Tb2-O8	0.237 4(6)		
O5A-Tb1-O11	92.7(2)	O11-Tb1-O12B	132.31(19)	O8-Tb2-O4D	141.8(2)
O5A-Tb1-O9	138.23(19)	O9-Tb1-O12B	139.70(18)	O4W-Tb2-O4D	75.5(2)
O11-Tb1-O9	80.7(2)	O1W-Tb1-O12B	81.9(2)	O6D-Tb2-O2W	86.2(3)
O5A-Tb1-O1W	84.7(3)	O1-Tb1-O12B	69.60(18)	O3E-Tb2-O2W	74.3(2)
O11-Tb1-O1W	142.9(2)	O7-Tb1-O12B	137.94(17)	O8-Tb2-O2W	70.7(2)
O9-Tb1-O1W	77.1(2)	O2-Tb1-O12B	94.59(18)	O4W-Tb2-O2W	143.8(3)
O5A-Tb1-O1	139.43(19)	O5A-Tb1-O12C	76.29(19)	O4D-Tb2-O2W	140.3(2)
O11-Tb1-O1	122.81(19)	O11-Tb1-O12C	65.96(17)	O6D-Tb2-O3W	150.8(2)
O9-Tb1-O1	72.57(18)	O9-Tb1-O12C	134.22(18)	O3E-Tb2-O3W	77.3(2)
O1W-Tb1-O1	77.8(2)	O1W-Tb1-O12C	146.8(2)	O8-Tb2-O3W	99.0(2)
O5A-Tb1-O7	72.76(19)	O1-Tb1-O12C	99.35(17)	O4W-Tb2-O3W	135.4(2)
O11-Tb1-O7	71.11(19)	O7-Tb1-O12C	124.80(18)	O4D-Tb2-O3W	79.0(2)
O9-Tb1-O7	66.06(18)	O2-Tb1-O12C	67.73(18)	O2W-Tb2-O3W	72.0(3)
O1W-Tb1-O7	72.9(2)	O12B-Tb1-O12C	66.57(19)	O6D-Tb2-O10	139.5(2)
O1-Tb1-O7	133.32(18)	O6D-Tb2-O3E	78.2(3)	O3E-Tb2-O10	138.6(2)
O5A-Tb1-O2	144.0(2)	O6D-Tb2-O8	91.6(2)	O8-Tb2-O10	66.98(18)
O11-Tb1-O2	71.55(18)	O3E-Tb2-O8	144.1(2)	O4W-Tb2-O10	69.8(2)
O9-Tb1-O2	72.59(19)	O6D-Tb2-O4W	73.1(3)	O4D-Tb2-O10	77.0(2)
O1W-Tb1-O2	127.4(2)	O3E-Tb2-O4W	127.4(2)	O2W-Tb2-O10	115.4(3)
O1-Tb1-O2	52.62(17)	O8-Tb2-O4W	80.3(2)	O3W-Tb2-O10	69.2(2)
O7-Tb1-O2	127.47(19)	O6D-Tb2-O4D	108.7(2)		
O5A-Tb1-O12B	71.89(19)	O3E-Tb2-O4D	73.3(2)		

Symmetry codes: A: *x*, *y*+1, *z*; B: *x*-1, *y*, *z*; C: -*x*+2, -*y*, -*z*; D: -*x*+1, -*y*-1, -*z*+1; E: -*x*+2, -*y*-1, -*z*+1.

2 Results and discussion

2.1 Synthesis

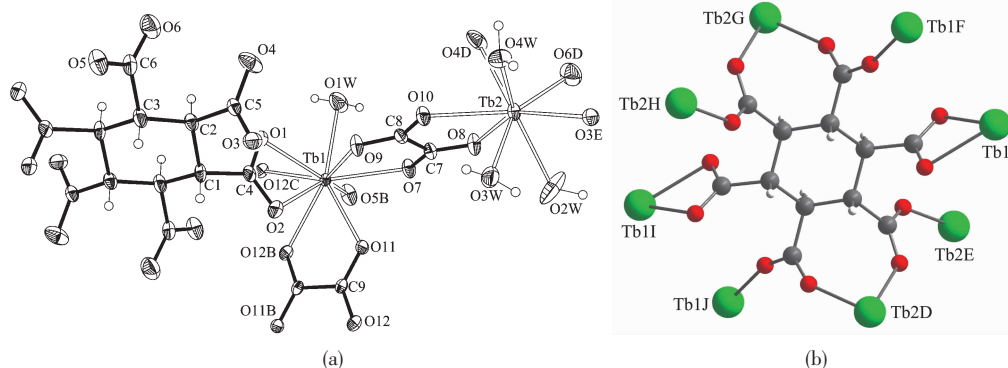
Hydrothermal synthesis is being widely used as a synthetic technique, not only for its advantageous preparation of highly stable metal-ligand frameworks, but also for its special reaction condition for the interesting reactions. It is well known that lanthanide ions are easily precipitated by oxalate, but under the condition of hydrothermal synthesis the preparation of new lanthanide frameworks containing both oxalate and other ligands is possible^[21-22]. In the formation of the title complex, it is of interest to note that the complex contains both rigid ox and the flexible cyclohexanepolycarboxylate ligands, which was rarely observed before for lanthanide frameworks.

From our previous studies on cyclohexanehexacarboxylic acid (H_6L), we observed that the size and versatile coordination environments of the metal ions, different alkali metal ions, the presence of auxiliary ligands and different reaction temperatures may play an important role in controlling the conformation of carboxylate groups on the cyclohexane ring^[14-19]. Considering the characters of lanthanide ions, we employed Tb(III) to react with the H_6L , attempting to trap the L ligand conformations (Scheme 1). As a result, the L^I in situ

transformed from the starting form L^I can be observed in the final crystal complex, proving that the Tb(III) with the presence of the ox ligand can also trap the L^II conformation of the cyclohexanehexacarboxylate ligand.

2.2 Structure of $[Tb_4(L^II)(ox)_3(H_2O)_8]$

X-ray diffraction crystal structure analysis reveals that the title complex is a three-dimensional framework crystallizing in $P\bar{1}$ space group. The asymmetric unit contains two crystallographically independent Tb (III) atoms, one L^II ligand transformed from the H_6L^I lying on a special position, two ox ligands, one of which lies on a special position, and four coordinated water molecules (Fig.1a). Tb1 adopts nine-coordinated geometry, with eight oxygen atoms from the L^II and ox ligands as well as a coordinated water molecule (Tb-O 0.227 4(5)~0.252 8(8) nm) (Table 2), presenting a geometry close to that of a monocapped square antiprism. Differently, Tb2 atom is eight-coordinated with five oxygen atoms from the L^II and ox ligands as well as three water molecules (Tb-O 0.229 8(6)~0.244 7(5) nm) (Table 2), giving a distorted bicapped trigonal prism geometry. The L^II ligand transformed from H_6L^I adopts μ_8 -bridging mode through its six *e*-carboxylate groups (Fig.1b), while the two kinds of ox ligands adopting μ_2 - and μ_4 -bridging modes, respectively.



Symmetry codes: A: $x, y+1, z$; B: $-x-1, y, z$; C: $-x+2, -y, -z$; D: $-x+1, -y-1, -z+1$; E: $-x+2, -y-1, -z+1$; F: $-x+1, -y, -z$; G: $x, y, z-1$; H: $x-1, y, z-1$; I: $-x+1, -y-1, -z$; J: $x, y-1, z$

Fig.1 (a) ORTEP drawing of coordination environment of the Tb atoms (with thermal ellipsoids at 50%); (b) Coordination mode of the L^II ligand

The μ_8 -bridging L^II ligands connect the Tb atoms to form a two-dimensional porous ($Tb-L^II$) layer extended through the *ab* plane (Fig.2a). The thickness of the layer is about 0.8 nm viewed along the *b* axis (Fig.2b).

There are two types of pores in the layers along the *c* axis (Fig.2a), distorted quadrangular pores with dimensions 0.55 nm×0.70 nm and elliptic pores with dimensions 0.62 nm×1.25 nm, respectively. Meanwhile,

there are one-dimensional channels with dimensions $0.65\text{ nm} \times 1.00\text{ nm}$ in the layers along the b axis (Fig. 2b). Meanwhile, the μ_2 - and μ_4 -bridging ox ligands

connect the Tb atom to form a one-dimensional (Tb-ox) chain. As showed in Fig.3a, the μ_4 -bridging ox ligands link the Tb1 atoms to make up the main (Tb-ox) chain,

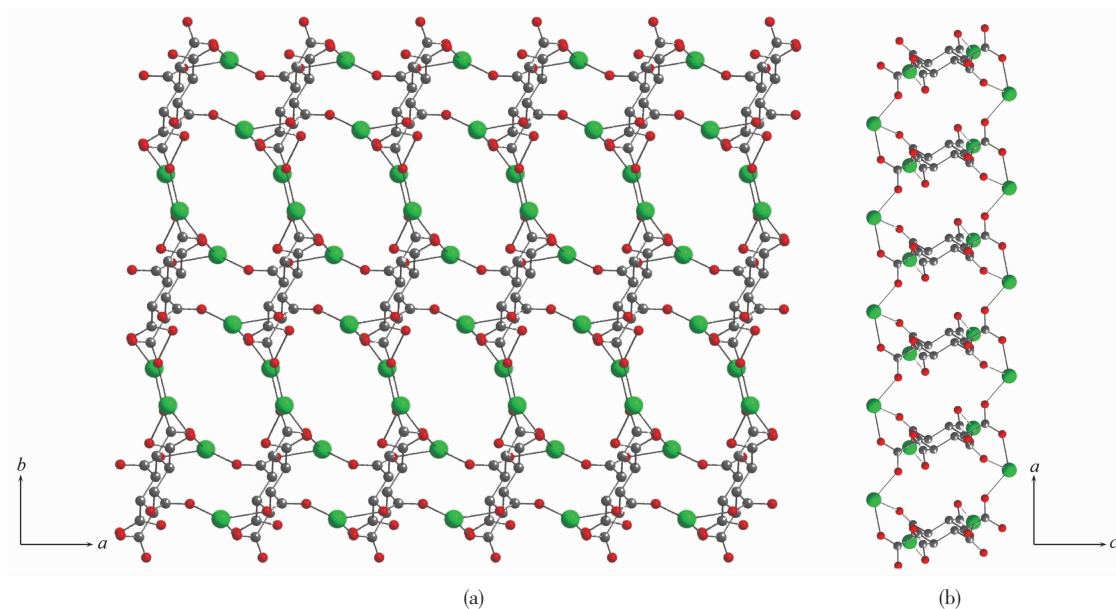


Fig.2 (a) Perspective views of the two-dimensional porous (Tb- L^{II}) layer bridged by the L^{II} ligand viewed along the c axis; (b) Along b axis

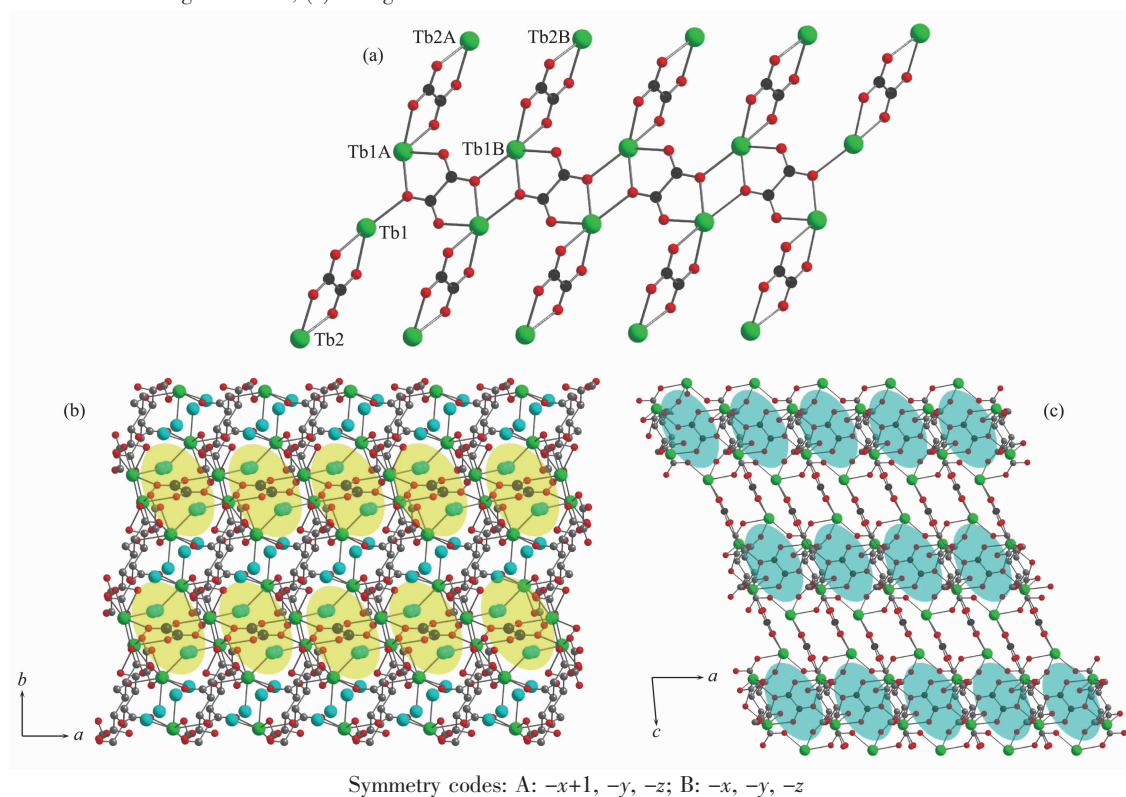


Fig.3 (a) Perspective views of the one-dimensional (Tb-ox) chain; (b) Three-dimensional framework bridged by L^{II} and ox ligands with elliptic channels occupied by ox ligand and water molecules viewed along the c axis; (c) Along b axis (yellow and blue ellipse shapes stand for the elliptic channels, and big blue balls in (b) stand for the water molecules)

and the μ_2 -bridging ox ligands link the Tb1 and Tb2 atoms to act as the decorations of the (Tb-ox) chain. Furthermore, the two-dimensional porous (Tb-L^{II}) layers are linked by the one-dimensional (Tb-ox) chains to generate a three-dimensional coordination framework with channels (Fig.3b,c).

It should be noted that the two kinds of elliptic channels in the framework are occupied by the μ_4 -

bridging ox ligands and coordinated water molecules, while the quadrangular are filled with coordinated water molecules (Fig.3b). Moreover, there are rich hydrogen interactions between the water molecules and the carboxylate groups of the L^{II} and ox ligands ($O \cdots O$ 0.267 4(8)~0.278 5(8) nm, $\angle O-H \cdots O$ 122(5)°~169(6)°) (Table 3), which further strengthen the three-dimensional framework.

Table 3 Hydrogen bond lengths and bond angles for the title complex

D-H \cdots A	d(D-H) / nm	d(H \cdots A) / nm	d(D \cdots A) / nm	\angle DHA / (°)
O1W-H1Wb \cdots O11A	0.086(2)	0.184(4)	0.267 4(8)	165(10)
O2W-H2Wa \cdots O8B	0.084(2)	0.214(5)	0.282 6(9)	139(6)
O3W-H3Wa \cdots O10C	0.085(2)	0.195(2)	0.278 5(8)	169(6)
O4W-H4Wb \cdots O1D	0.085(2)	0.216(6)	0.270 8(8)	122(5)

Symmetry codes: A: $x-1, y, z$; B: $-x+2, -y, -z+1$; C: $-x+2, -y-1, -z+1$; D: $-x+1, -y-1, -z+1$.

References:

- [1] Bradshaw D, Claridge J B, Cussen E J, et al. *Acc. Chem. Res.*, **2005**,**38**:273-282
- [2] Ye B H, Tong M L, Chen X M. *Coord. Chem. Rev.*, **2005**,**249**:545-565
- [3] Zhao B, Chen X Y, Cheng P, et al. *J. Am. Chem. Soc.*, **2004**,**126**:15394-15395
- [4] Bunzli J C G, Piguet C. *Chem. Soc. Rev.*, **2005**,**34**:1048-1077
- [5] Zhang M B, Zhang J, Zheng S T, et al. *Angew. Chem., Int. Ed.*, **2005**,**44**:1385-1388
- [6] Cheng J W, Zhang J, Zheng S T, et al. *Angew. Chem., Int. Ed.*, **2006**,**45**:73-76
- [7] Shi W, Chen X, Zhao Y, et al. *Chem. Eur. J.*, **2005**,**11**:5031-5039
- [8] Sun Y Q, Zhang J, Yang G Y. *Chem. Commun.*, **2006**:1947-1949
- [9] Chui S S Y, Lo S M F, Charmant J P H, et al. *Science*, **1999**,**283**:1148-1150
- [10] Humphrey S M, Wood P T. *J. Am. Chem. Soc.*, **2004**,**126**:13236-13237
- [11] PENG Meng-Xia(彭梦侠), CHEN Zi-Yun(陈梓云). *Chinese J. Inorg. Chem.(Wuji Huaxue Xuebao)*, **2009**,**25**(6):1055-1061
- [12] Bi W, Cao R, Sun D, et al. *Chem. Commun.*, **2004**:2104-2105
- [13] Kitagawa S, Uemura K. *Chem. Soc. Rev.*, **2005**,**34**:109-119
- [14] Wang J, Hu S, Tong M L. *Eur. J. Inorg. Chem.*, **2006**:2069-2077
- [15] Wang J, Zheng L L, Li C J, et al. *Cryst. Growth Des.*, **2006**,**6**:357-359
- [16] Wang J, Zhang Y H, Tong M L. *Chem. Commun.*, **2006**:3166-3168
- [17] Wang J, Lin Z J, Ou Y C. *Chem. Eur. J.*, **2008**,**24**:7218-7235
- [18] Wang J, Ou Y C, Shen Y, et al. *Cryst. Growth Des.*, **2009**,**9**:2442-2450
- [19] WANG Jing(王静), LIU Zhao-Qing(刘兆清). *Chinese J. Inorg. Chem.(Wuji Huaxue Xuebao)*, **2010**,**26**(11):2077-2082
- [20] Sheldrick G M. *SADABS 2.05*, University of Göttingen, **2000**.
- [21] SHELXTL 6.10, *Bruker Analytical Instrumentation*, Madison, Wisconsin, USA, **2000**.
- [22] Song J L, Mao J G. *Chem.-Eur. J.*, **2005**,**11**:1417-1424
- [23] Zhu W H, Wang Z M, Gao S. *Inorg. Chem.*, **2007**,**46**:1337-1342